Computation of Effective Mechanical Properties and Mechanical Erosion Modeling of TPS Materials

Sergio Fraile Izquierdo, Jeremie B.E. Meurisse, Federico Semeraro, Georgios Bellas Chatzigeorgis, Marcos Acín, Nagi N. Mansour

Analytical Mechanics Associates, Inc. at NASA Ames Research Center

Presented by
Sergio Fraile Izquierdo

Thermal & Fluids Analysis Workshop
TFAWS 2022
September 6th-9th, 2022
Virtual Conference

Outline

- Motivation: TPS Solid Mechanics at Different Scales
- Computation of Effective Mechanical Properties
  - Introduction to PuMA
  - Micro-mechanics Model
  - Multi-scale Modeling of TPS Composites
    - Porous Matrix, Fibers/Tows, Unit Cell
  - Validation Case: 3D Woven TPS
- Mechanical Erosion Modeling of TPS Materials
  - Introduction to PATO
  - Mechanical Erosion Model
  - Stress Analysis Solver Implementation
  - Solver Validation Cases
  - Failure Criteria and Mass Removal Model
- Conclusions and Future Work

3D weave structure

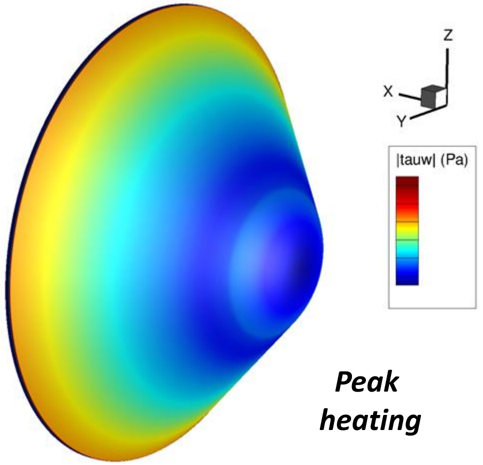

Shear stress during atmospheric entry

Motivation: TPS Solid Mechanics at different scales

- Solid mechanics simulations of TPS materials allow us to understand their mechanical performance during entry.
- TPS mechanical properties are needed for the full-scale models, these can be obtained through micro-mechanics modeling of the material’s microstructure.
- This modeling process leverages two frameworks developed at NASA:
  - The Porous Microstructure Analysis (PuMA) Software [1].
  - The Porous material Analysis Toolbox based on OpenFOAM (PATO) [2].

Macroscale / Full scale

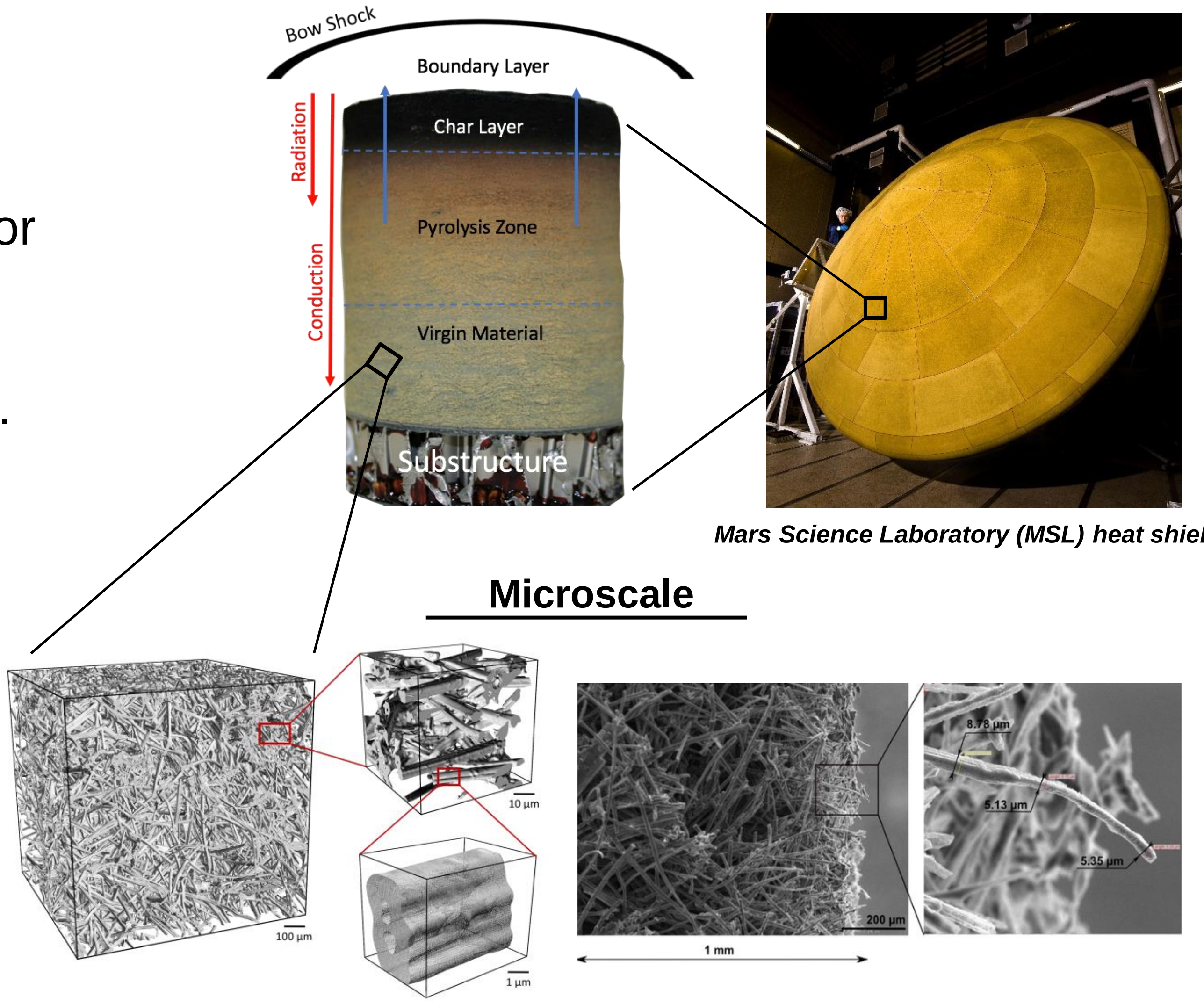

Mars Science Laboratory (MSL) heat shield

Carbon-fiber microstructure

Motivation: TPS Solid Mechanics at different scales

- Solid mechanics simulations of TPS materials allow us to understand their mechanical performance during entry.
- TPS mechanical properties are needed for the full-scale models, these can be obtained through micro-mechanics modeling of the material's microstructure.
- This modeling process leverages two frameworks developed at NASA:
  - The Porous Microstructure Analysis (PuMA) Software [1].
  - The Porous material Analysis Toolbox based on OpenFOAM (PATO) [2].

Macroscale / Full scale

PATO

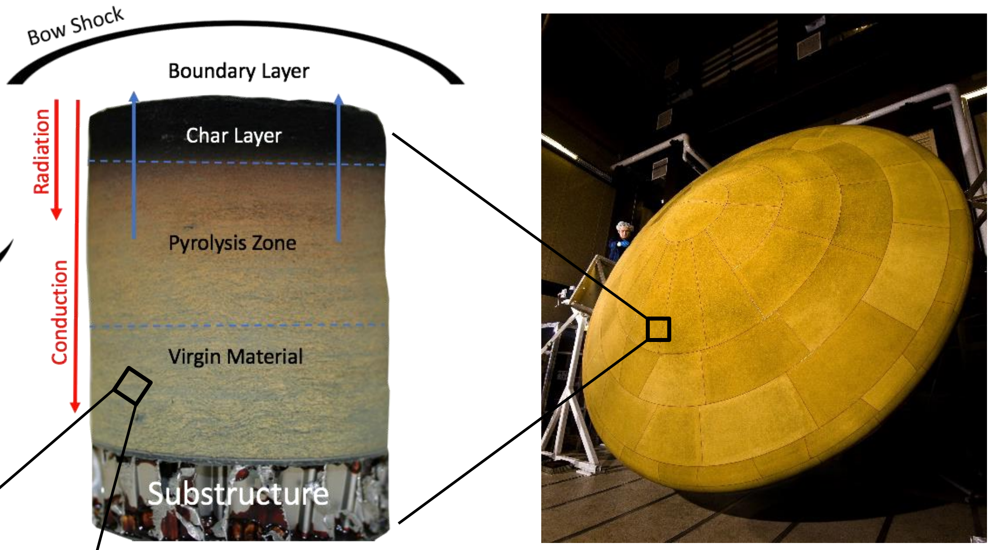

Mars Science Laboratory (MSL) heat shield

Microscale

PuMA

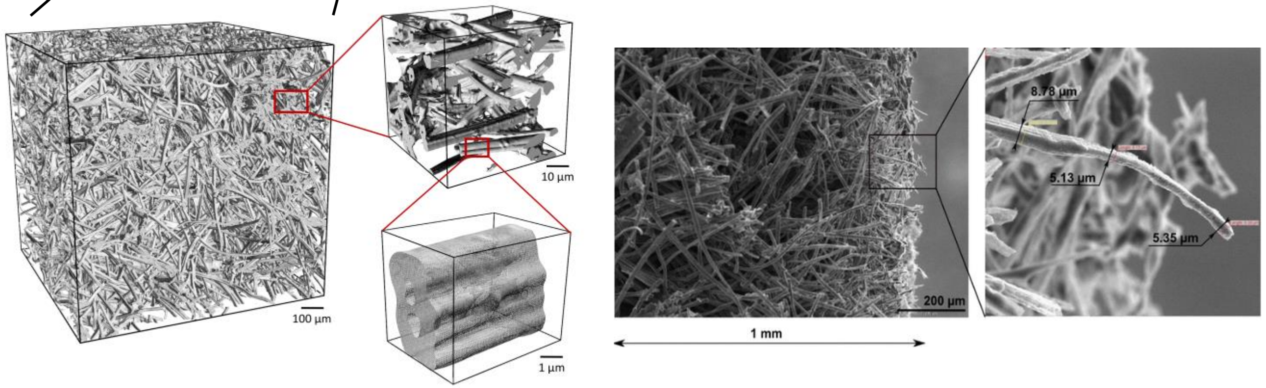

Carbon-fiber microstructure

Introduction to PuMA

- The PuMA software is able to either generate domains artificially or import them from micro-CT scans and compute material properties such as: porosity, specific surface area, effective thermal conductivity, pore diameter, tortuosity, permeability. It also enables the computation of mechanical properties though its anisotropic elasticity solver.

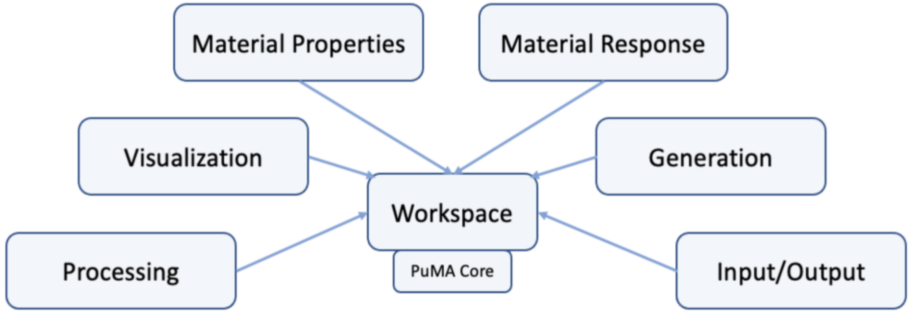

Porous Microstructure Analysis (PuMA)

Domain Generation

- X-ray Microtomography import / filtering
- Woven Material Generation (TexGen)
- Simplified Geometry Generation
  - Analytical shapes
  - Fibrous Materials
  - Sphere Beds
  - Triply Periodic Materials

Material Properties

- Porosity / Volume Fractions
- Specific Surface Area
- Pore Diameter
- Effective Thermal & Electrical Conductivity
- Anisotropic Thermal & Electrical Conductivity
- Anisotropic Elasticity
- Material Orientation
- Continuum Tortuosity
- Rarefied Tortuosity
- Permeability

Shared Utilities

- Matrix & Vector data structures / operations
- Linear Solvers
- Iso-surface extraction
- Input/output utilities

Material Response

- Microscale Oxidation
- Hyperthermal Beam Simulations

● Included in open-source release
○ Not included in open-source release

Introduction to PuMA

- **Lead developers:** J.C. Ferguson and F. Semeraro
- **Installation:** conda install -c conda-forge puma
- **Open-source repository:** https://github.com/nasa/puma
- **Documentation:** https://puma-nasa.readthedocs.io
- **Community chat:** https://gitter.im/puma-nasa/community
- **Tutorials:** YouTube channel and Colab notebook

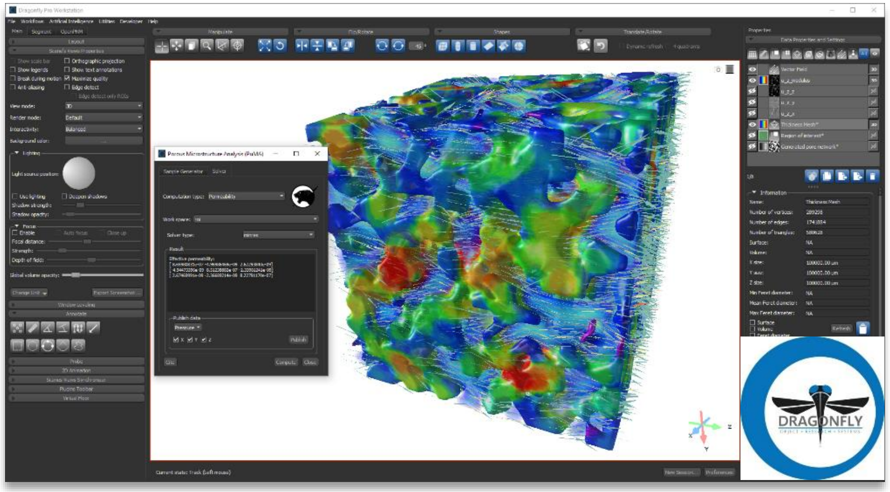

Dragonfly software using PuMA

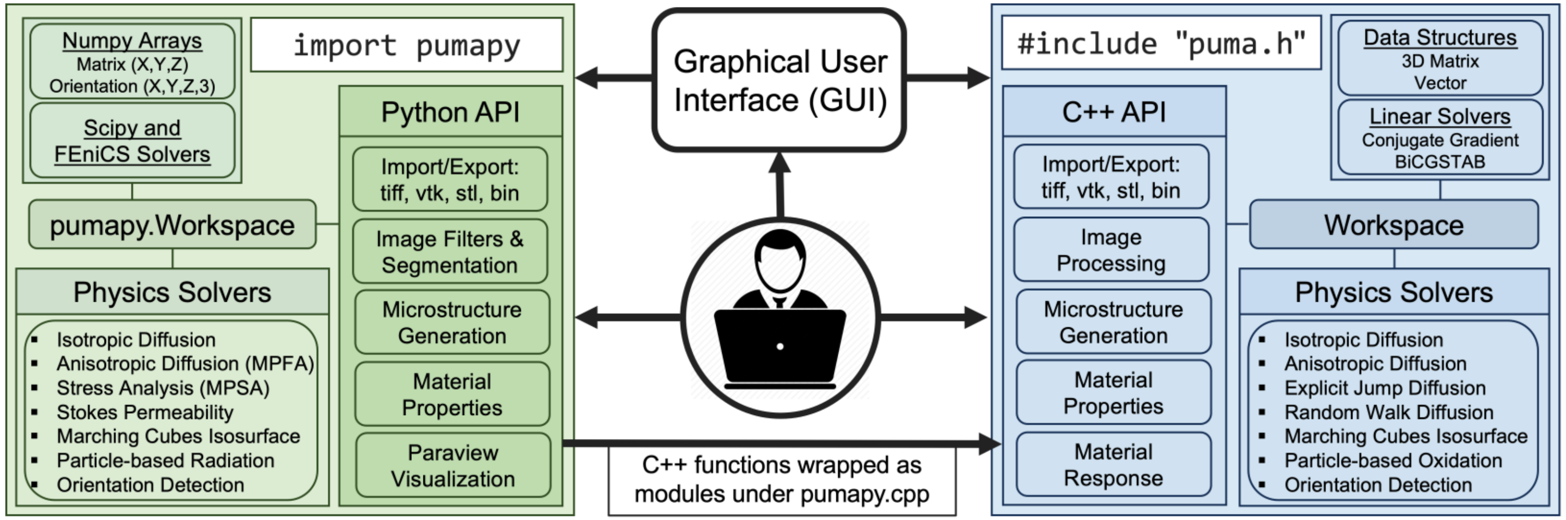

PuMA architecture diagram

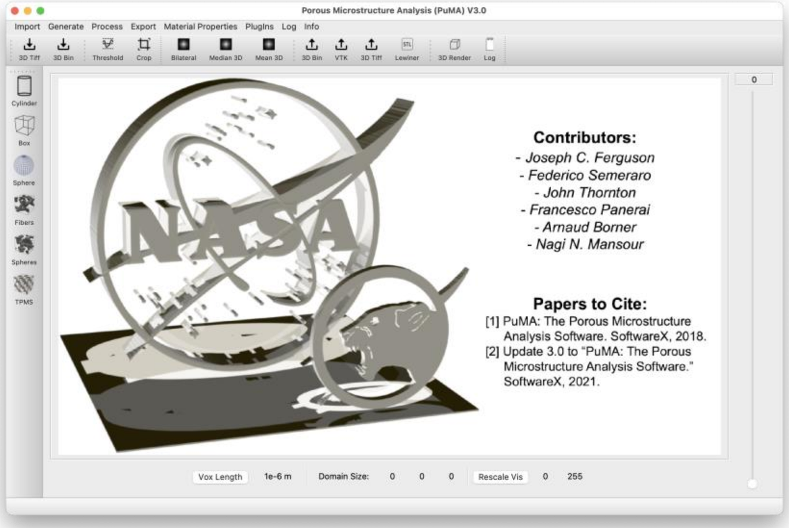

PuMA GUI

Introduction to Pu

- **Lead developers:** J.C. Ferguson and F. Semeraro
- **Installation:** conda install -c conda-forge puma
- **Open-source repository:** https://github.com/nasa/pum
- **Documentation:** https://puma-nasa.readthedocs.io
- **Community chat:** https://gitter.im/puma-nasa/communi
- **Tutorials:** YouTube channel and Colab notebook

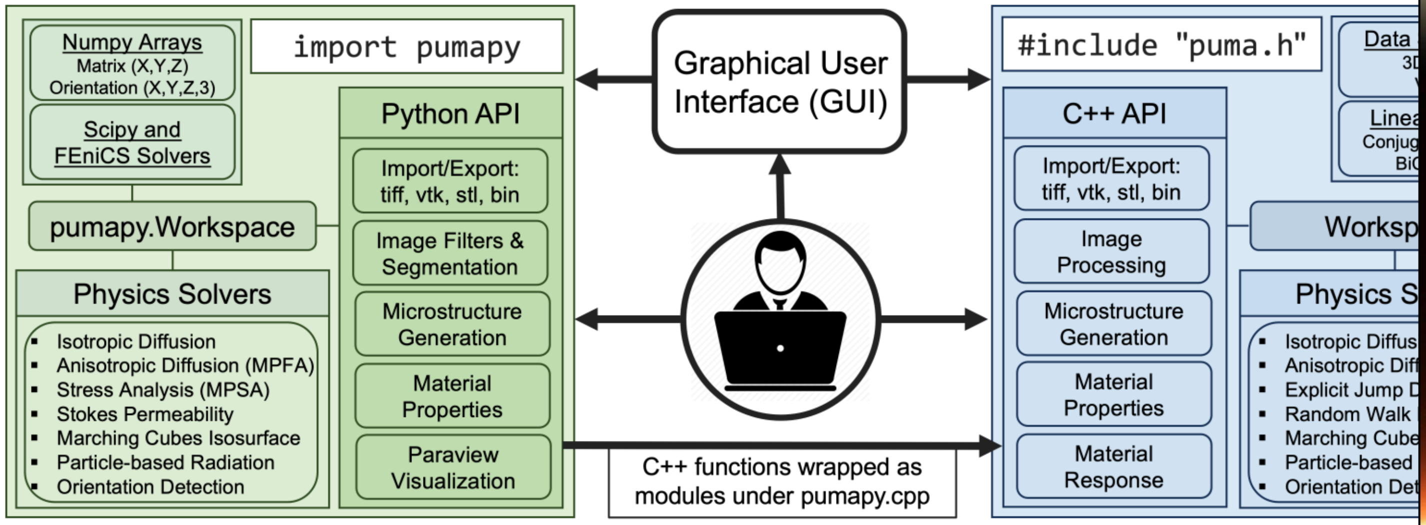

PuMA architecture diagram

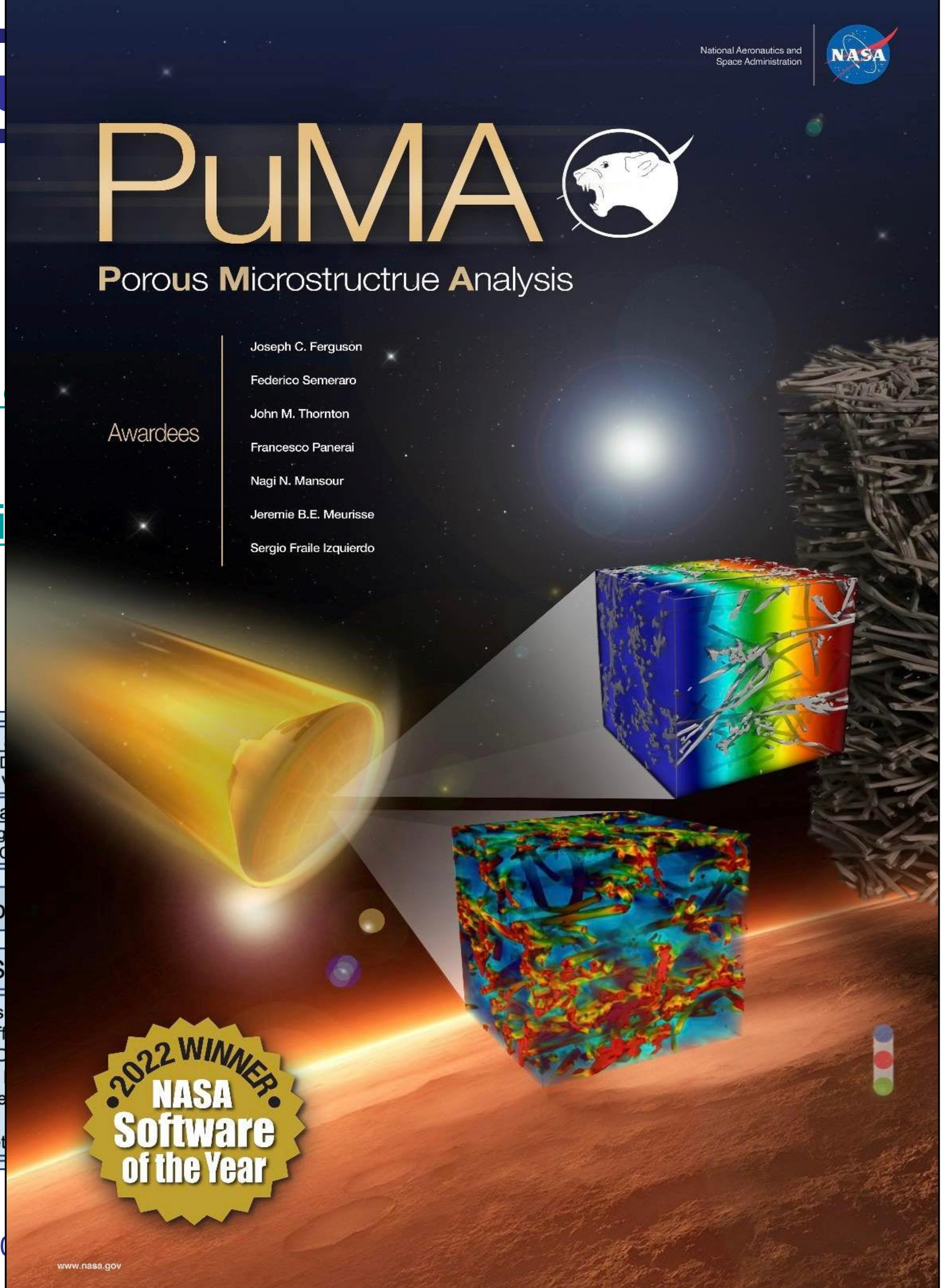

Micro-mechanics Model

- This presentation focuses on multi-scale modeling to obtain the mechanical properties TPS materials.
- Modeling steps: Matrix → Tows → Unit Cell
- TPS optimization: constituents' selection, resin infusion process, curing process, yarns' structure, fiber volume fraction…
- PuMA's voxel-based stress analysis solver for anisotropic linear elastic materials:
  - Finite volume
  - Cell-centered discretization
  - Cell-face stress values obtained with the MPSA-W method [3,4]

$$\nabla \cdot \boldsymbol{\sigma} = 0 \quad \text{where}$$

$$\boldsymbol{\sigma} = \boldsymbol{C\varepsilon} = \begin{bmatrix} C^{11} & C^{12} & C^{13} & C^{14} & C^{15} & C^{16} \\ C^{12} & C^{22} & C^{23} & C^{24} & C^{25} & C^{26} \\ C^{13} & C^{23} & C^{33} & C^{34} & C^{35} & C^{36} \\ C^{14} & C^{24} & C^{34} & C^{44} & C^{45} & C^{46} \\ C^{15} & C^{25} & C^{35} & C^{45} & C^{55} & C^{56} \\ C^{16} & C^{26} & C^{36} & C^{46} & C^{56} & C^{66} \end{bmatrix} \frac{\nabla \boldsymbol{u} + (\nabla \boldsymbol{u})^T}{2}$$

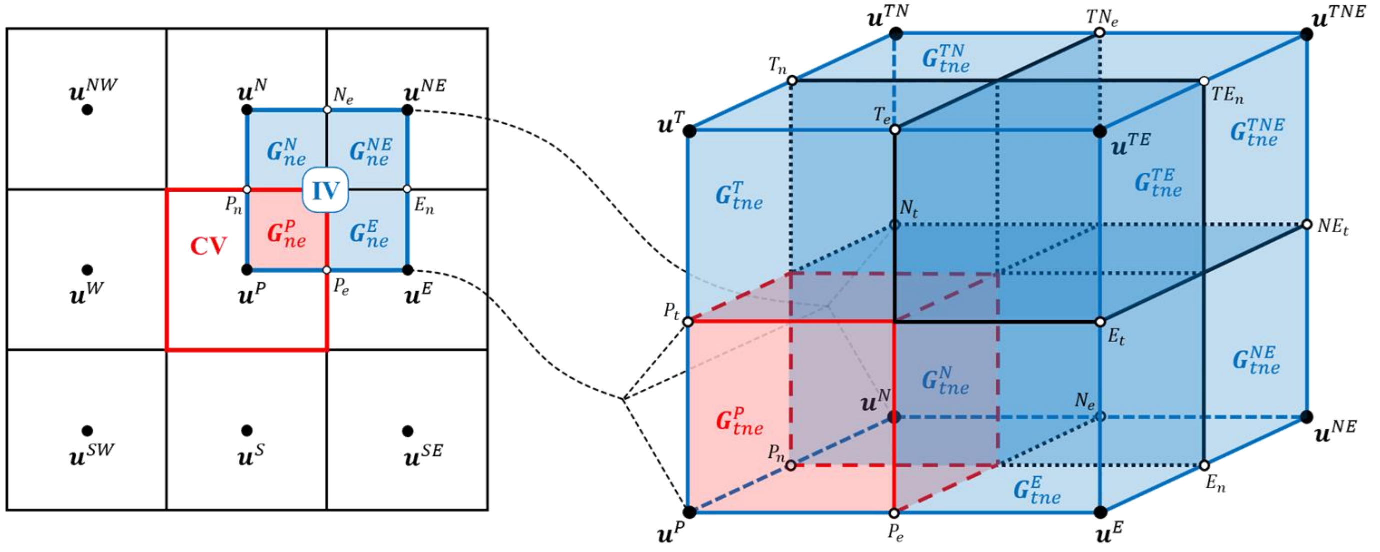

Micro-mechanics Model

- Effective mechanical properties obtained with PuMA following the Representative Volume Element (RVE) homogenization method [5,6]:
  - Run a simulation for each principal direction (3 total) imposing a known displacement on each face while keeping the opposite face fixed.
  - Symmetry or periodic boundary conditions for the other 4 faces.
  - Solve the stress field generated in the material and obtain the anisotropic elasticity tensor C.
  - Assuming isotropic or orthotropic behavior, it is possible to obtain from C the effective Young's modulus E, and the Poisson's ratio ν.
- Similar approach can be used for the pure shear cases.

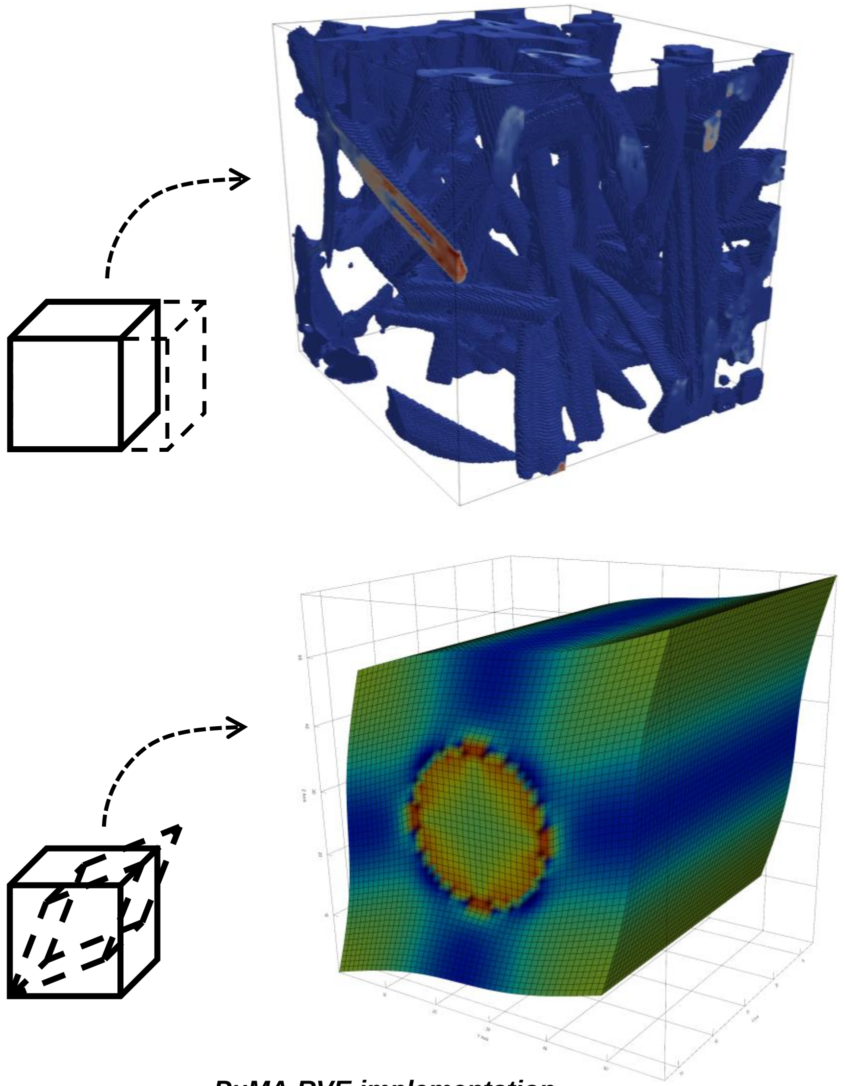

PuMA RVE implementation

Multi-scale Modeling of TPS Composites

S. Fraile Izquierdo, F. Semeraro, M. Acín, 2022. Multi-Scale Analysis of Effective Mechanical Properties of Porous 3D Woven Composite Materials. *AIAA Scitech Forum*

Matrix: porous phenolic resin

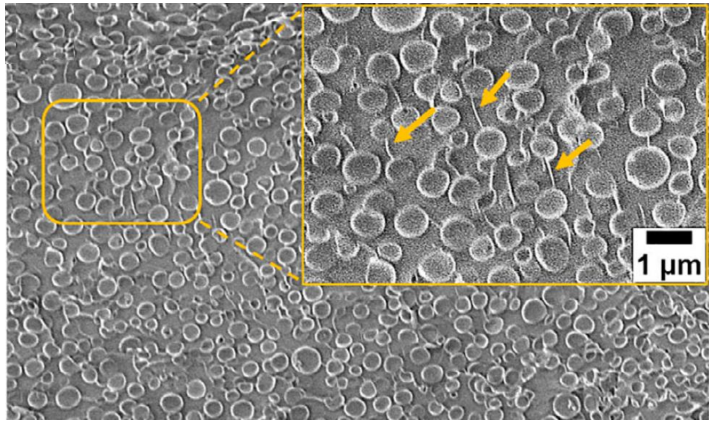

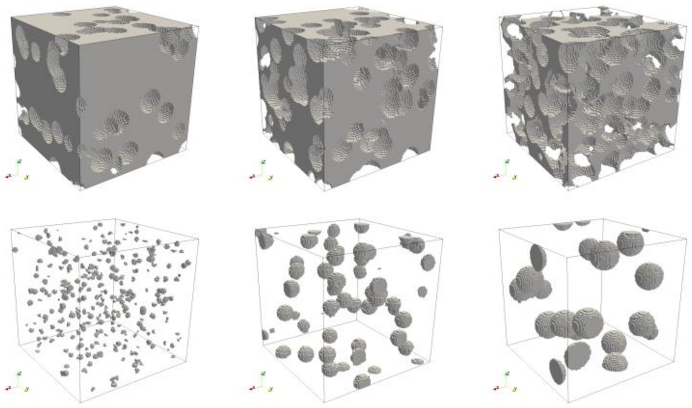

Validated with **Bert's** [7] and **Roberts'** [8] semi-empirical equations that follow the structure:

$$E_\phi = E_0 \left(1 - \frac{\phi}{\phi_{max}}\right)^c$$

Intra-tow fiber packing

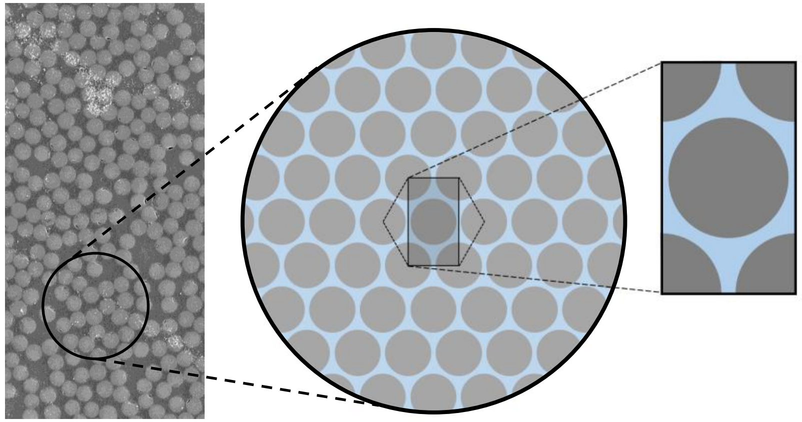

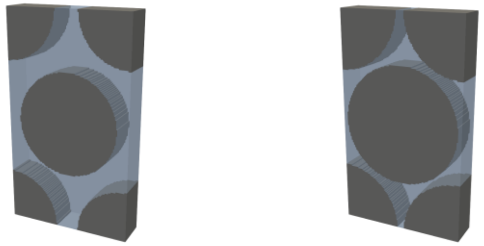

ROM [9] $E_L = E_{f_L} V_f + E_m V_m$ $\nu_{LT} = \nu_{f_{LT}} V_f + \nu_m V_m$

Halpin-Tsai Nielsen [10,11] $E_T = E_m \frac{1 + \xi \eta V_f}{1 - \psi \eta V_f}$ *where,* $\eta = \frac{r-1}{r+\xi}$ $r = \frac{E_{f_T}}{E_m}$

Chamis [12] $E_T = \frac{E_m}{1 - \sqrt{V_f}\left(1 - \frac{E_m}{E_{f_T}}\right)}$

TPS unit cell

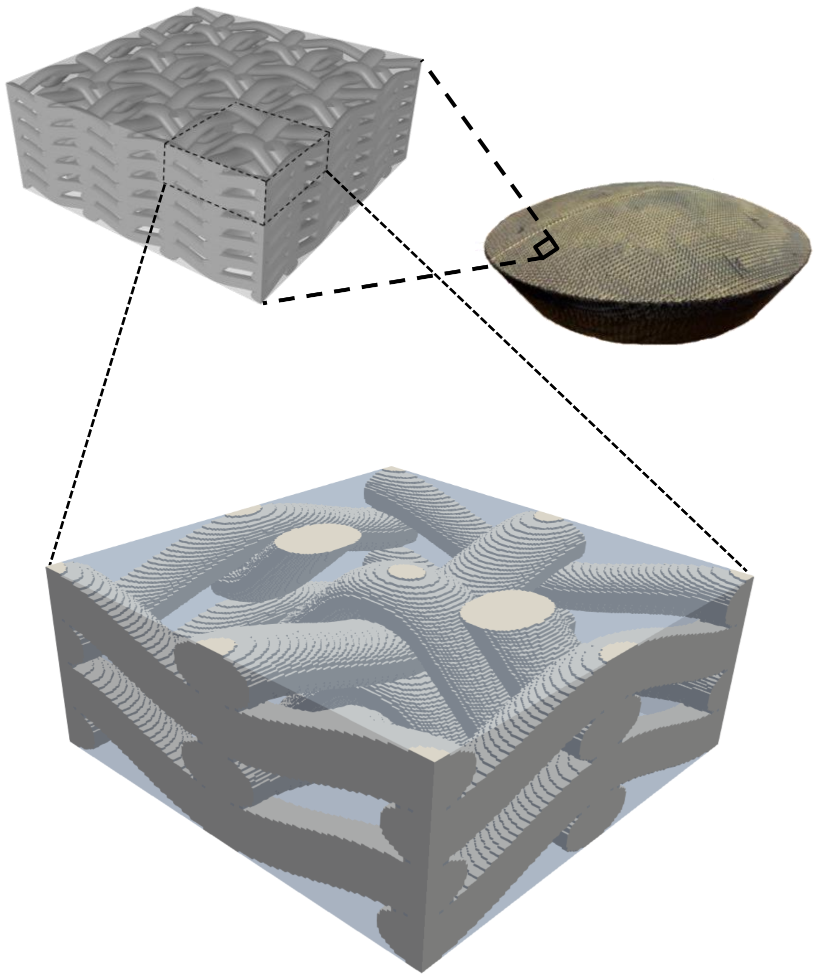

Validation Case: 3D Woven TPS

Matrix: porous phenolic resin

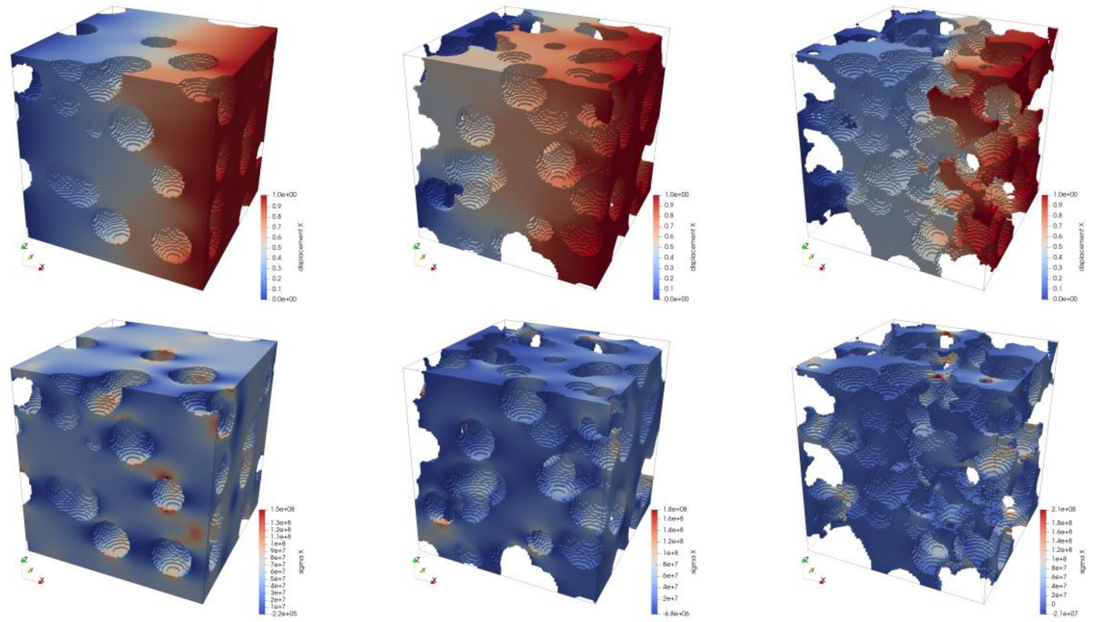

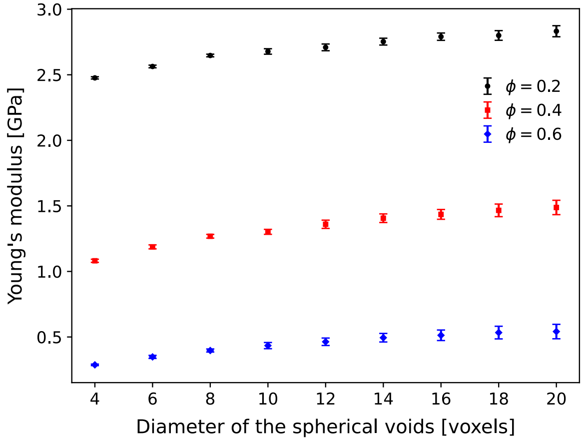

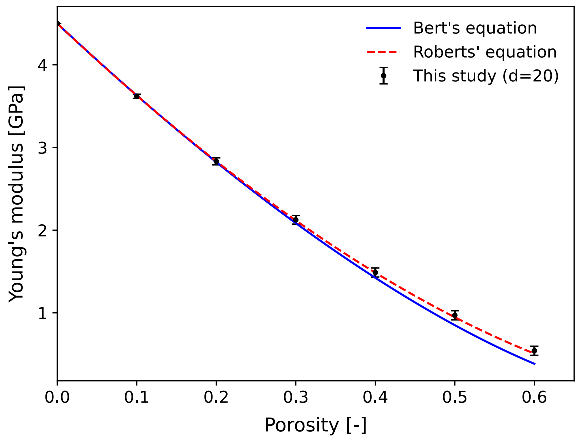

Intra-tow fiber packing

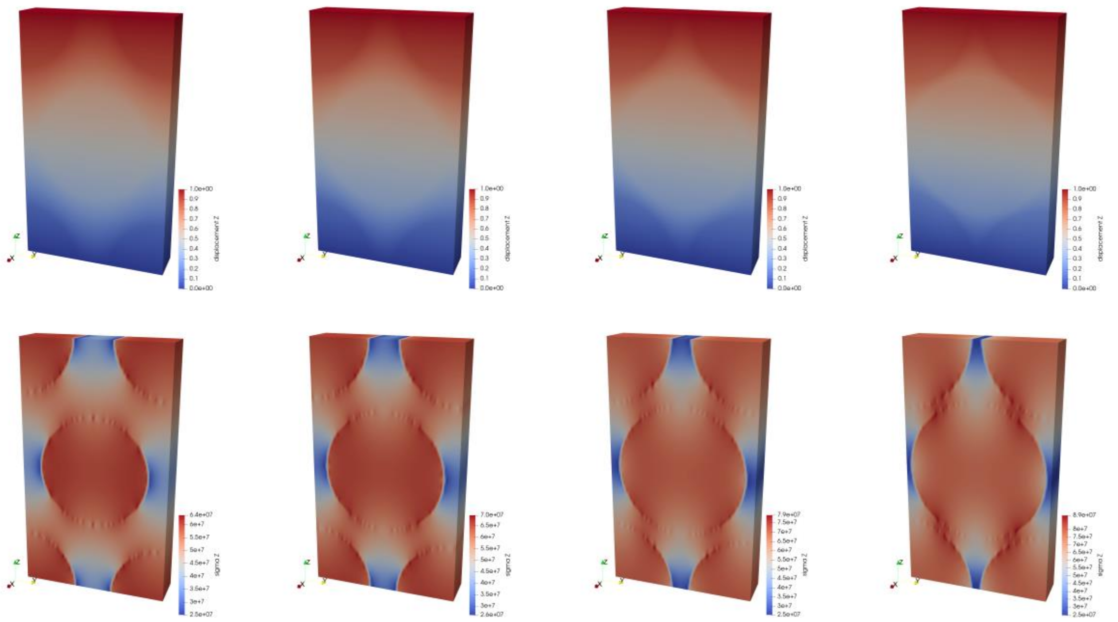

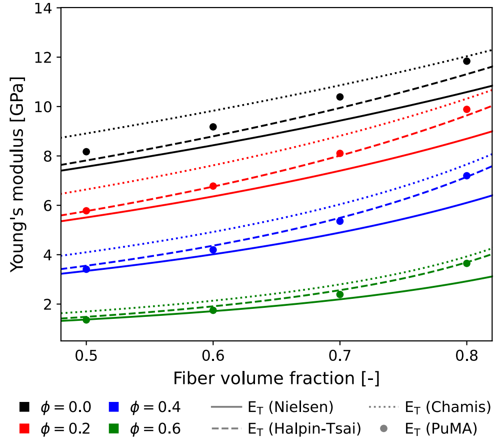

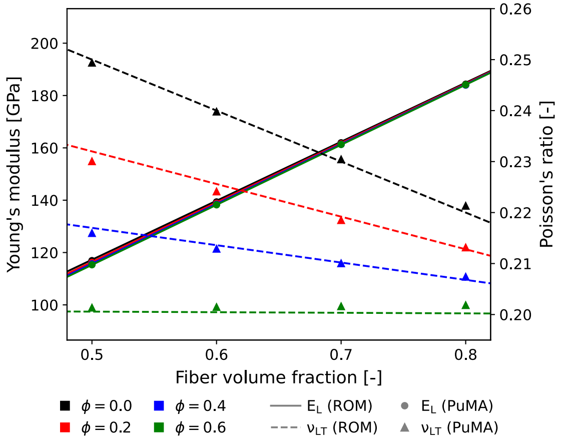

Validation Case: 3D Woven TPS

TPS unit cell

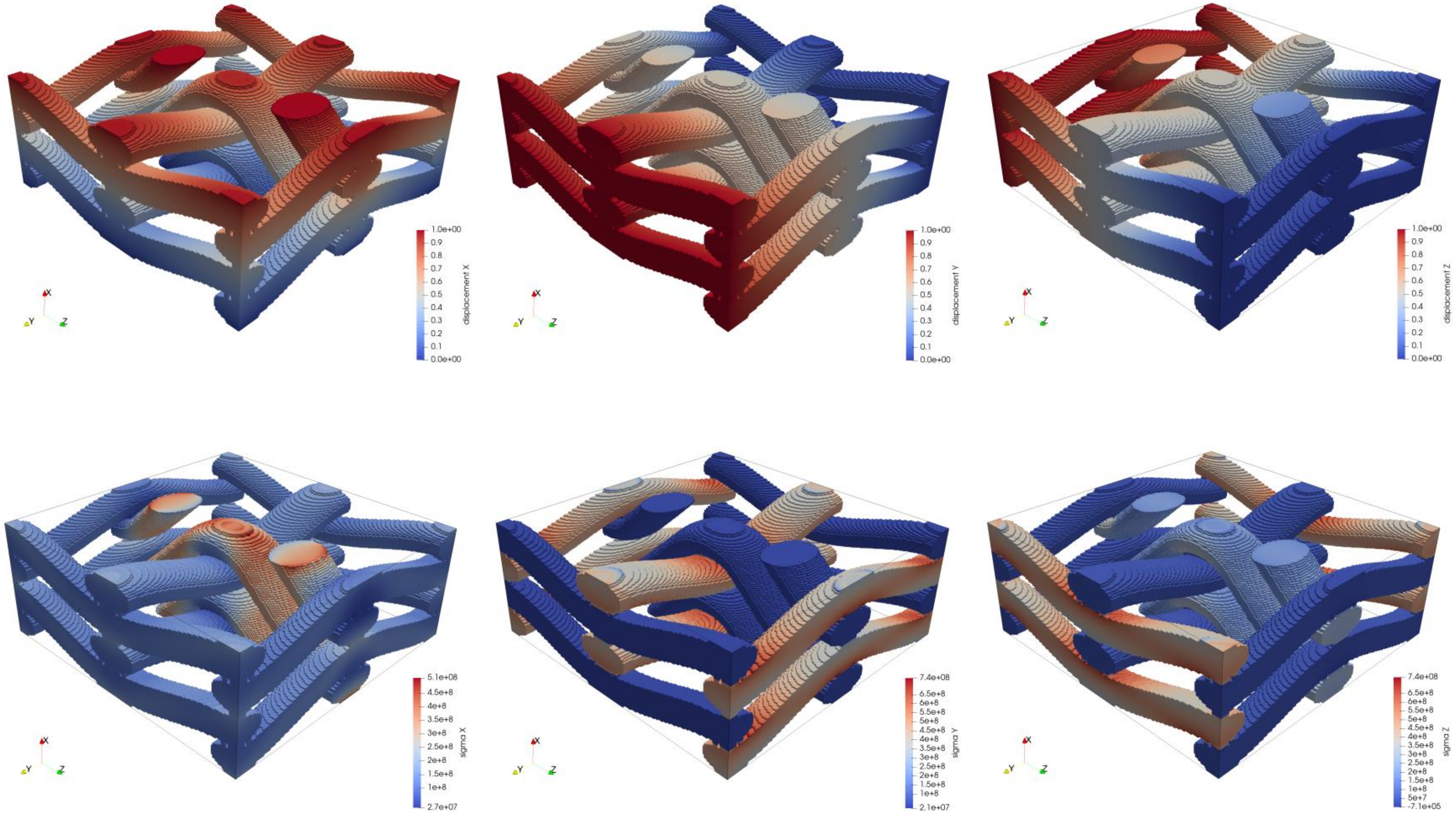

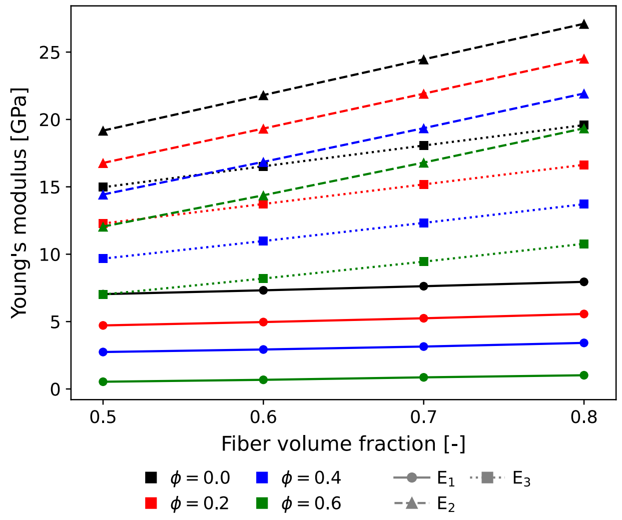

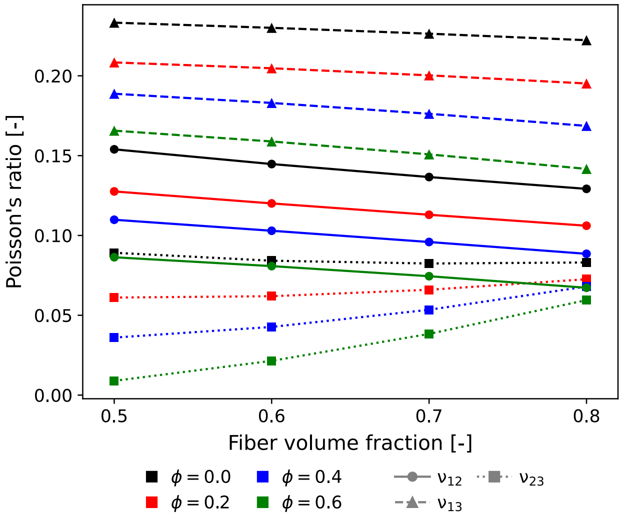

Introduction to PATO

- PATO is an open-source software for Computational Material Response of reactive porous materials submitted to high-enthalpy environments [13].
- Enables modeling most of the atmospheric entry material response physics to refine estimates of mission risks:
  - Equilibrium / Finite-rate chemistry / Multi-material
  - Ablation / Pyrolysis / Heat conduction
- Recent advancements [14]:
  - Coupling with CFD
  - PICA-NuSil Modeling
  - Unified Solver
  - Mechanical Erosion Modeling
- The Mechanical Erosion Model relies on the mechanical properties computed with PuMA.

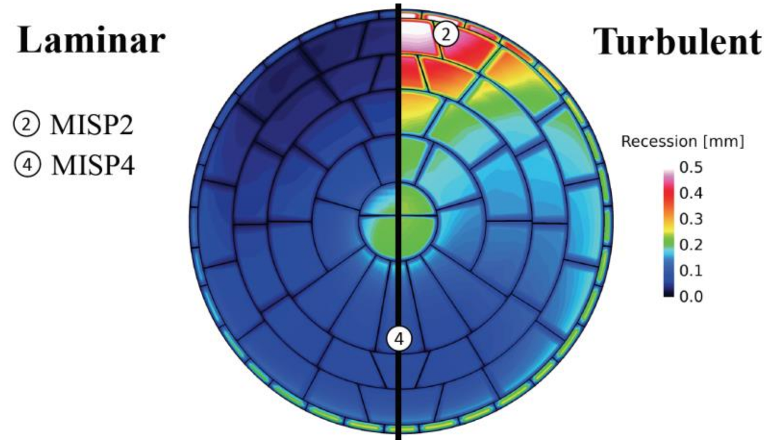

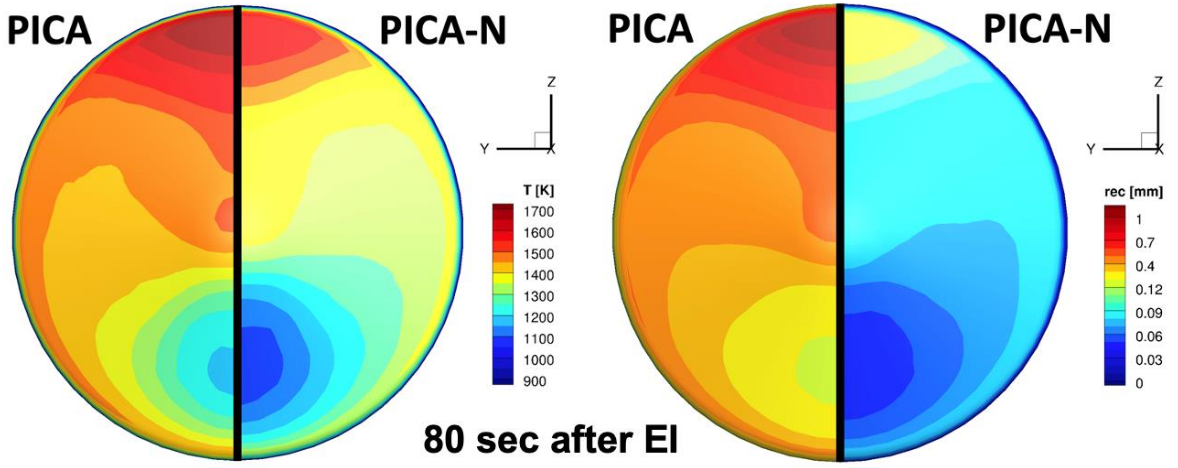

PATO full-heatshield simulations

Introduction to PATO

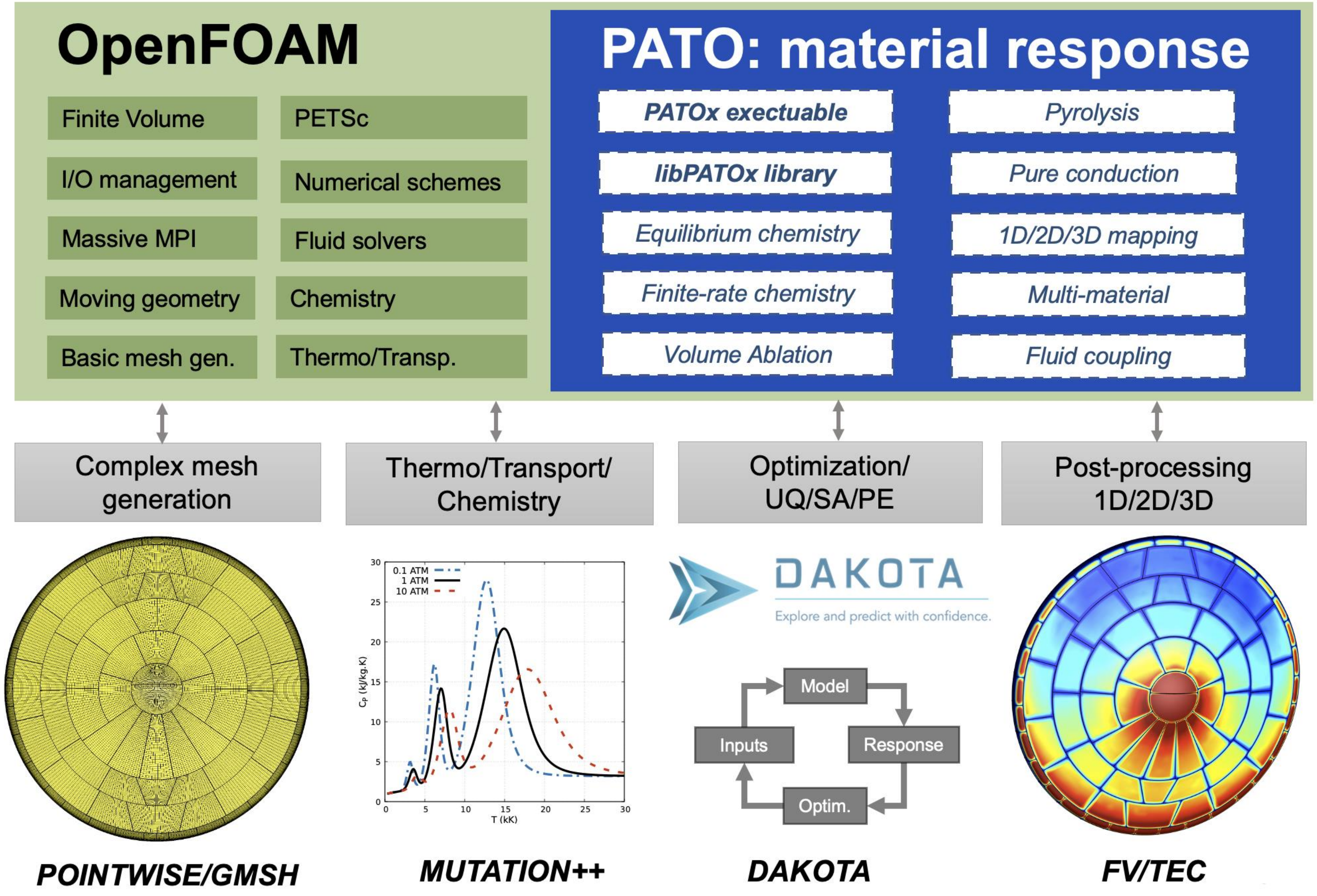

PATO architecture diagram

- **Point of contact:**
  - Jeremie B.E Meurisse
- **PATO website:**
  - https://pato.ac/
- **PATO module on PFE**
  - module use –a /u/jmeuriss/modulefiles
  - module load PATO/dev
  - module load dakota/6.7
  - module load cmake/3.9
- **1D, 2D, 3D tutorials on PFE**
  - /u/jmeuriss/sharing/PATO/PATO-dev/tutorials
- **Development repository:**
  - https://gitlab.com/PATO/PATO-dev
- **Open-source repository:**
  - https://github.com/nasa/pato

Mechanical Erosion Model

- The goal of this work is to model the mechanical response of TPS materials during atmospheric entry.
- Determine if there is additional surface recession in Thermal Protection Systems (TPS) materials as a result of mechanical erosion due loads and thermal effects during atmospheric entry:
  - External forces on the heatshield's surface: shear stress and pressure from the flow field
  - Thermal stress induced by the material's temperature field
  - Normal stress induced by pyrolysis gas build-up
  - Shrinkage due to pyrolysis of the material
- These same physics also apply to intumescent gap-filler materials such as RTV, which are important to understand to model the differential recession between the TPS material and the gap-filler.

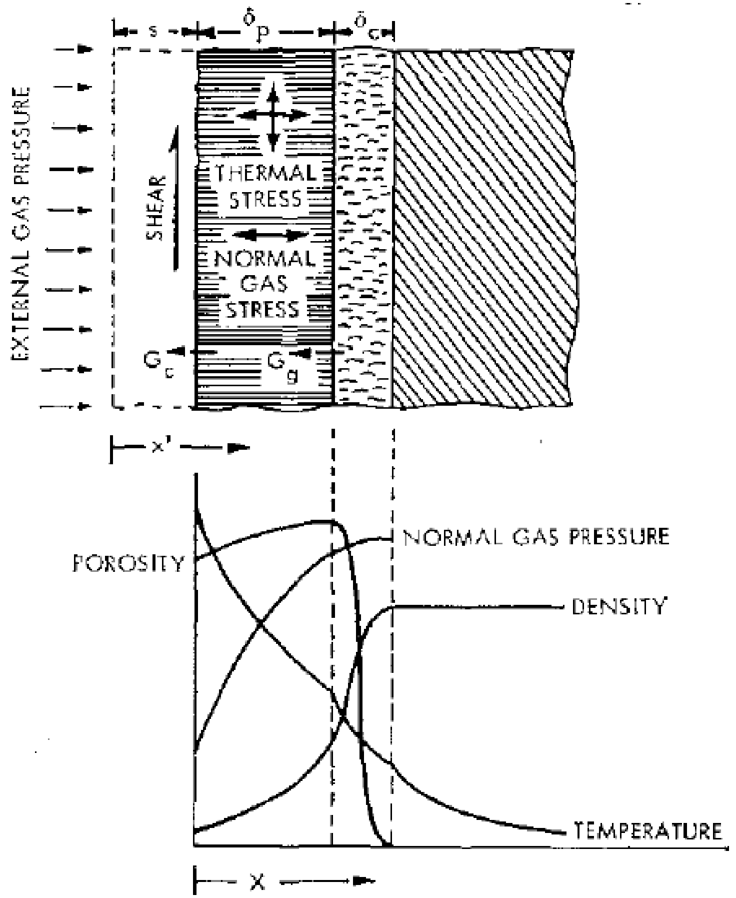

Thermal mechanics of charring ablators [15]

Mechanical Erosion Model

DPLR

Aerothermal environment Hypersonic CFD

p_w h_r C_H $\overline{\overline{\tau_w}}$

PATO

Material response solver → Update mechanical properties → Stress analysis solver → Failure criteria model → Mass removal model

T $\dot{s}$

Hypersonic CFD computed using DPL. The aero-thermal environment: wall pressure [p_w], recovery enthalpy [h_r] and heat transfer coefficient [C_H]) are extracted from Blayer. The wall shear stress tensor [$\overline{\overline{\tau_w}}$] is extracted from the Postflow utility.

This PATO solver computes the pressure (Darcy's flow) and the temperature inside the material as well as the surface recession.

The mechanical properties (E, G, nu and CTE) are updated as a function of the material temperature and orientation.

This solver computes the stress tensor and the displacement for orthotropic materials using the CFD wall shear stress tensor.

These models define the regions where the stress is higher than the ultimate strength and then move the mesh accordingly.

The mechanical removal model coupled with the material response solvers is able to predict the total recession $\dot{s}$ in the material due to surface chemistry and mechanical erosion

Stress Analysis Solver Implementation

- Assuming small strains and small rotations, the conservation of linear momentum solved in PATO follows [16,17]:

$$\frac{\partial}{\partial t}\int_{\Omega_0}\rho\,\frac{\partial u}{\partial t}\,\mathrm{d}\Omega_0 = \overbrace{\oint_{\Gamma_0} n_0\cdot(K\cdot\nabla u)\,\mathrm{d}\Gamma_0}^{\text{Implicit Term}} + \overbrace{\oint_{\Gamma_0} n_0\cdot\sigma\,\mathrm{d}\Gamma_0 - \oint_{\Gamma_0} n_0\cdot(K\cdot\nabla u)\,\mathrm{d}\Gamma_0}^{\text{Explicit Terms}} + \int_{\Omega_0}\rho\, b\,\mathrm{d}\Omega_0$$

- Where $K\cdot\nabla u$ is an approximation of the stress field in terms of the displacement field. This segregated solution approach allows to solve the governing equation independently for each direction. Outer iterations are performed until the explicit terms change less than some predefined tolerance; in that case, the first and third terms on the right-hand side "cancel out" and the calculated displacement field satisfies the governing equation.

- Orthotropic constitutive law for material: the 81 terms of the elastic stiffness tensor, C, can be reduced to nine independent material parameters:

$$C_{ijkl} = f(E_1, E_2, E_3, G_1, G_2, G_3, \nu_{12}, \nu_{23}, \nu_{31})$$

$$\begin{bmatrix}\sigma_{11}\\ \sigma_{22}\\ \sigma_{33}\\ \sigma_{12}\\ \sigma_{23}\\ \sigma_{31}\end{bmatrix} = \begin{bmatrix} C_{11} & C_{12} & C_{31} & 0 & 0 & 0\\ C_{12} & C_{22} & C_{23} & 0 & 0 & 0\\ C_{31} & C_{23} & C_{33} & 0 & 0 & 0\\ 0 & 0 & 0 & C_{44} & 0 & 0\\ 0 & 0 & 0 & 0 & C_{55} & 0\\ 0 & 0 & 0 & 0 & 0 & C_{66}\end{bmatrix}\begin{bmatrix}\epsilon_{11}-\alpha_{11}\Delta T\\ \epsilon_{22}-\alpha_{22}\Delta T\\ \epsilon_{33}-\alpha_{33}\Delta T\\ \epsilon_{12}\\ \epsilon_{23}\\ \epsilon_{31}\end{bmatrix}$$

- The discretized equation for each control volume P can be written in the form of an algebraic equation:

$$a_P\, u_P - \sum_{f=1}^{F} a_{N_f}\, u_{N_f} = b_P \xrightarrow{\textbf{Assembled for all CVs}} [A][U] = [B]$$

Solver Validation Cases

- The analytical solution of the stress σ around the circumference of the hole derived by Lekhnitskii [18] has been used by different authors to validate their models [19,20]. To validate the orthotropic stress analysis implemented in PATO, the test case shown below was used which consists of a plate of 8 x 8 with a hole radius of 0.5 and 70,405 hexahedron elements.

Properties	Values
E_x	10, 30, 50 GPa
E_y	10, 30, 50 GPa
G_{xy}	8 GPa
ν_{xy}	0.25

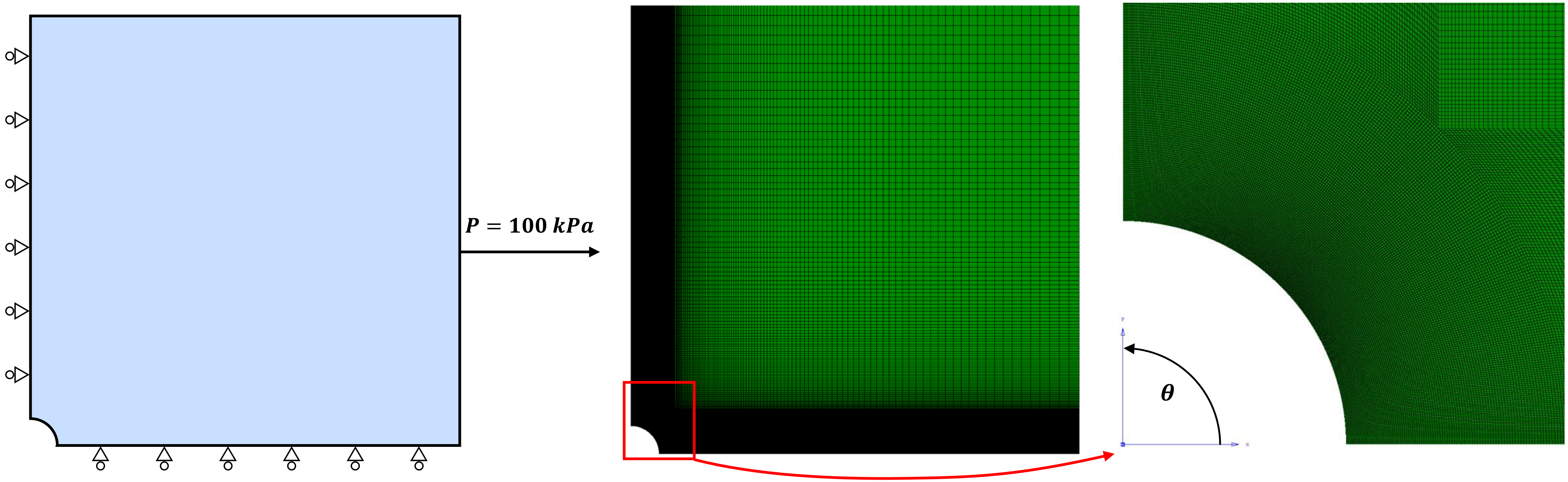

Detail of the model (left) and mesh structure (right) for the Orthotropic Plate with a Hole validation case

σ_{xx}

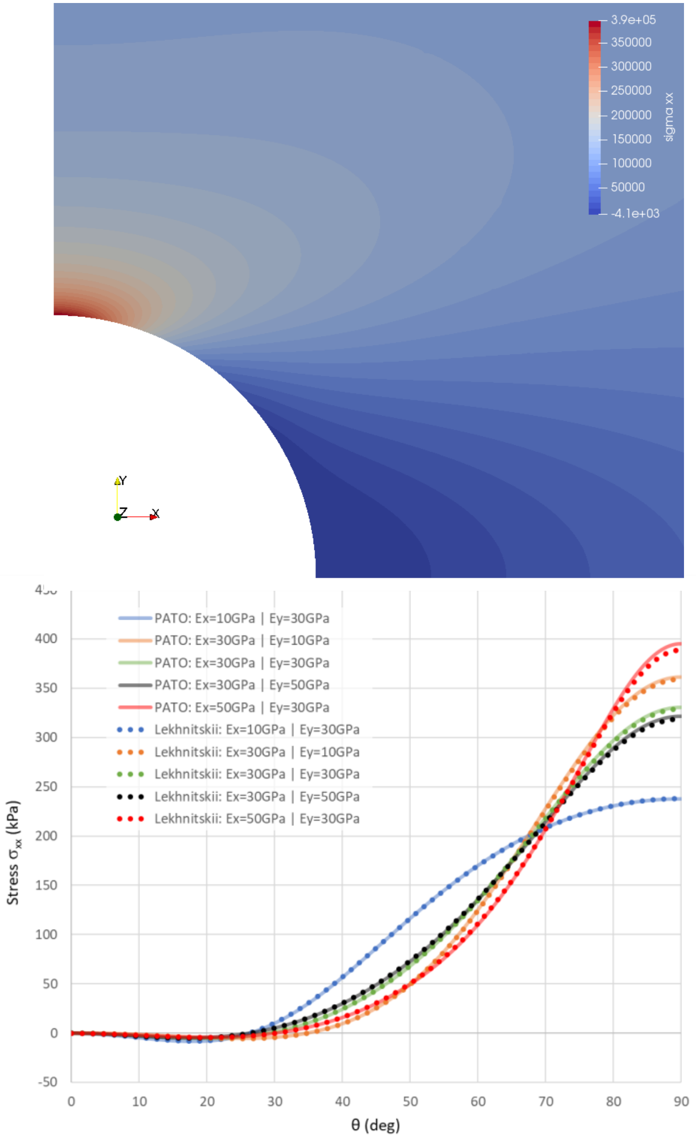

σ_{yy}

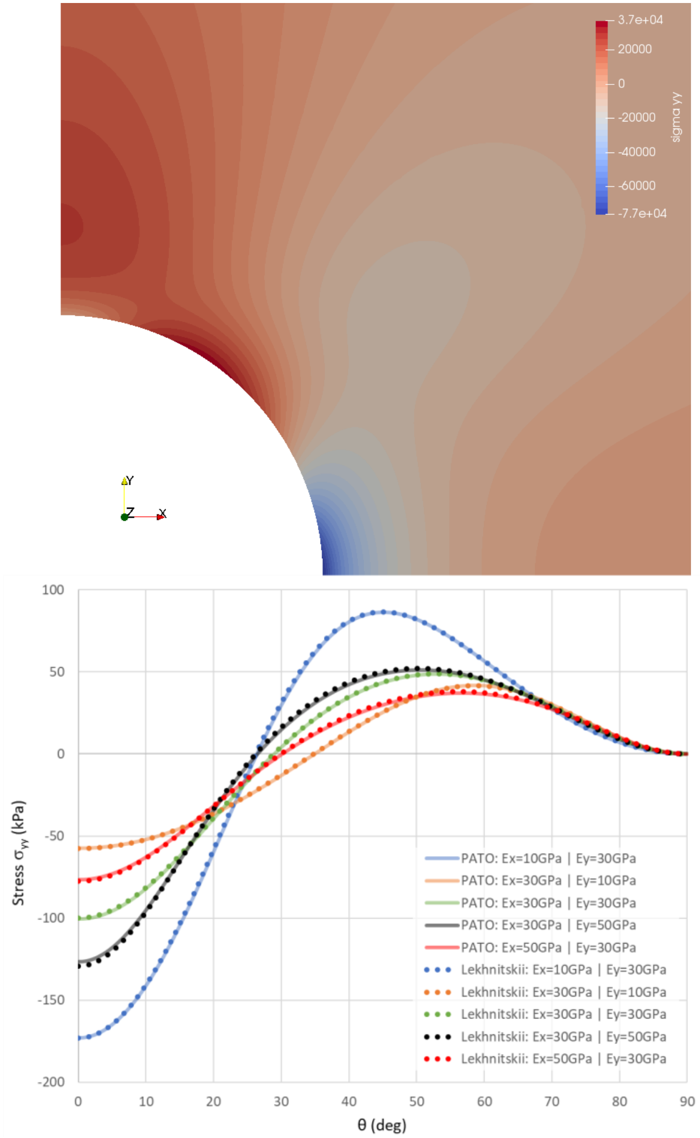

σ_{xy}

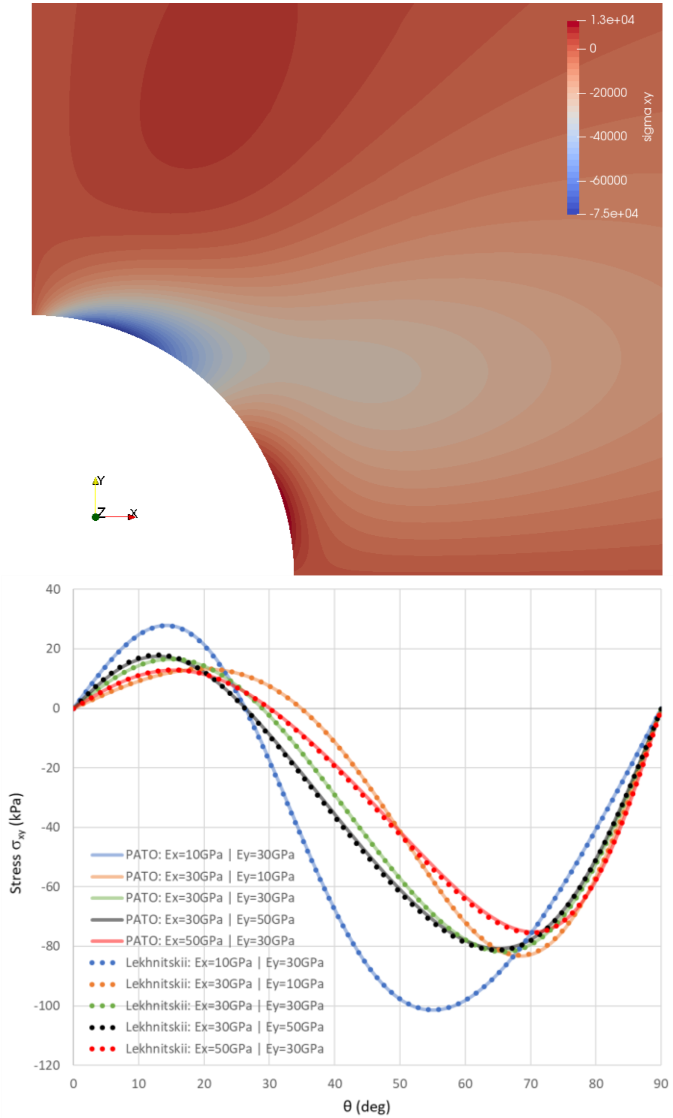

Solver Validation Cases

- To validate the orthotropic thermal stress implementation, a cube (0.5 x 0.5 x 0.5 m) shaped mesh made of 125,000 hexahedron elements was used with the following mechanical properties and boundary conditions:

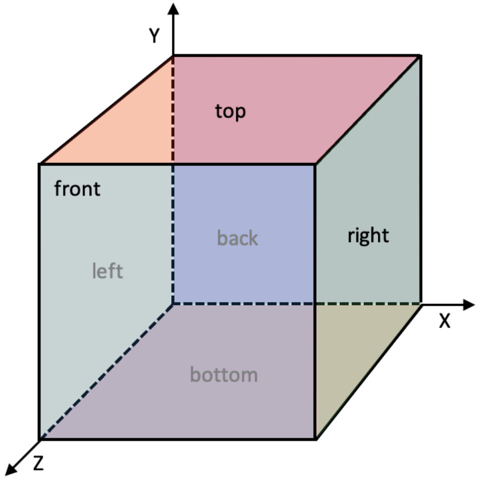

- Constant $T = 300\ K$, $T_0 = 100\ K$
- Acceleration = $[9800\ 0\ 0]\ m/s^2$
- $\alpha_{ortho} = [2 \cdot 10^{-5}\quad 4 \cdot 10^{-5}\quad 6 \cdot 10^{-5}]\ K^{-1}$
- $\nu_{xy} = 0.15$, $\nu_{yz} = 0.20$, $\nu_{xz} = 0.25$
- $E_x = 6\ GPa$, $E_y = 3\ GPa$, $E_z = 1\ GPa$
- $G_{xy} = 0.9\ GPa$, $G_{yz} = 0.6\ GPa$, $G_{xz} = 0.4\ GPa$

- Results were compared against FEA solutions [21].

σ_{xx} (Error$_{max}$ = 0.005%)

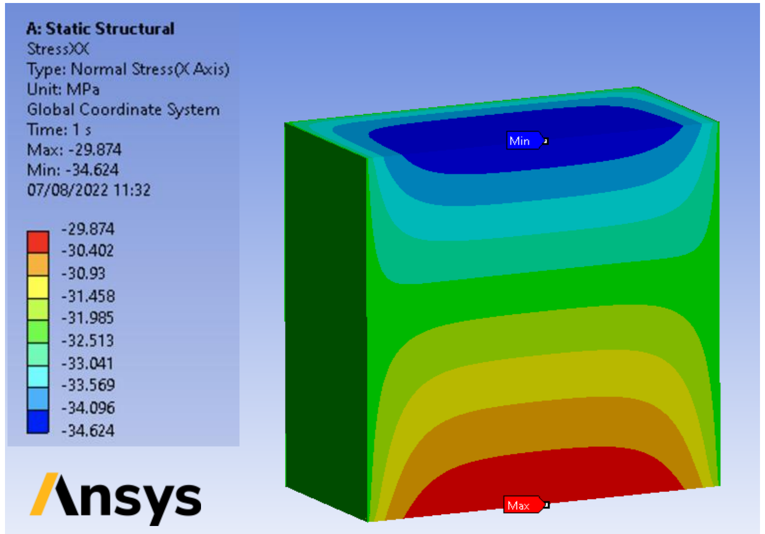

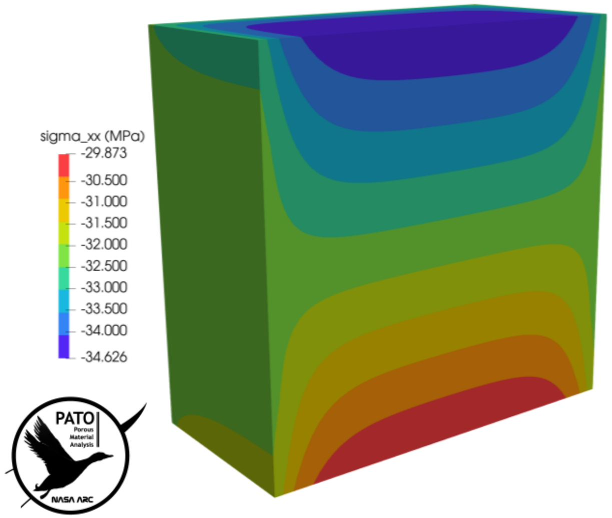

Solver Validation Cases

σ_{yy} ($Error_{max}$ = 0.006%)

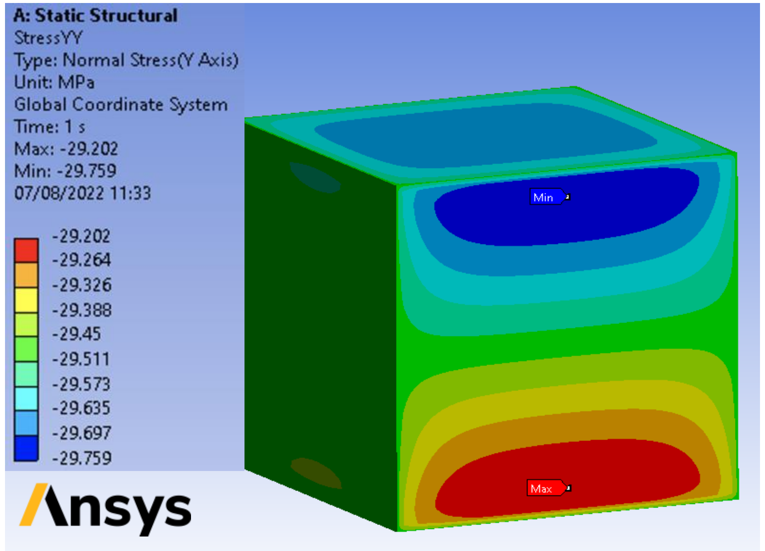

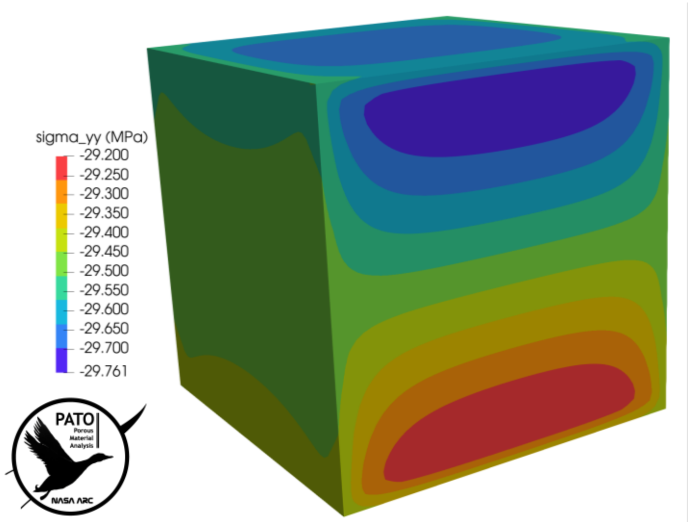

σ_{zz} ($Error_{max}$ = 0.025%)

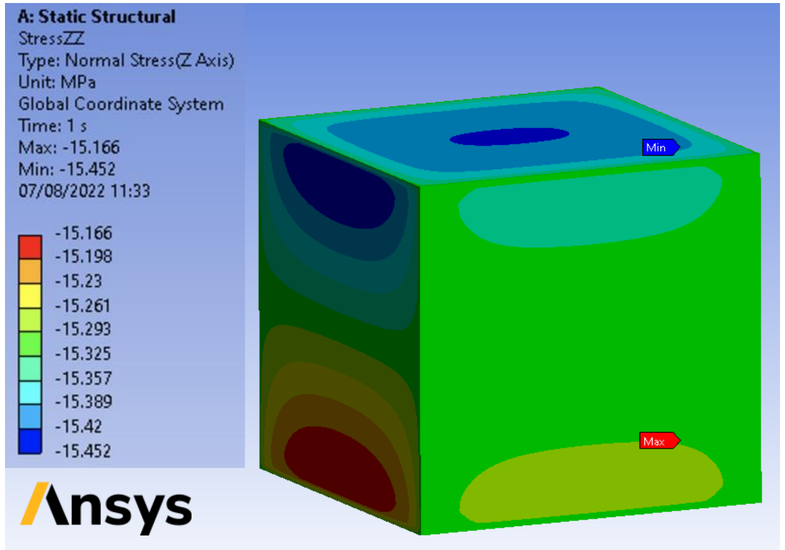

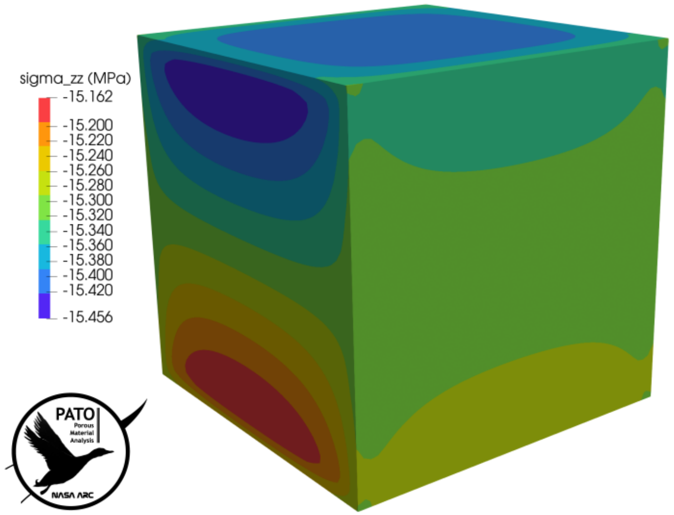

σ_{yz} ($Error_{max}$ = 0.057%)

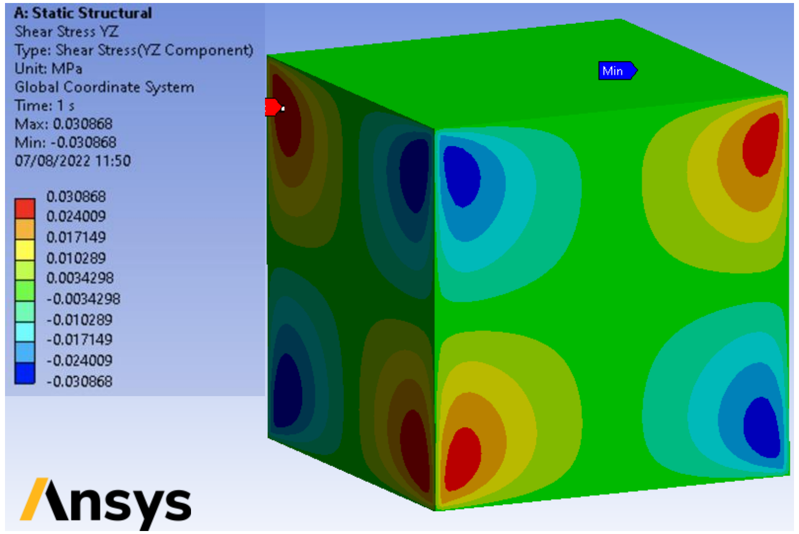

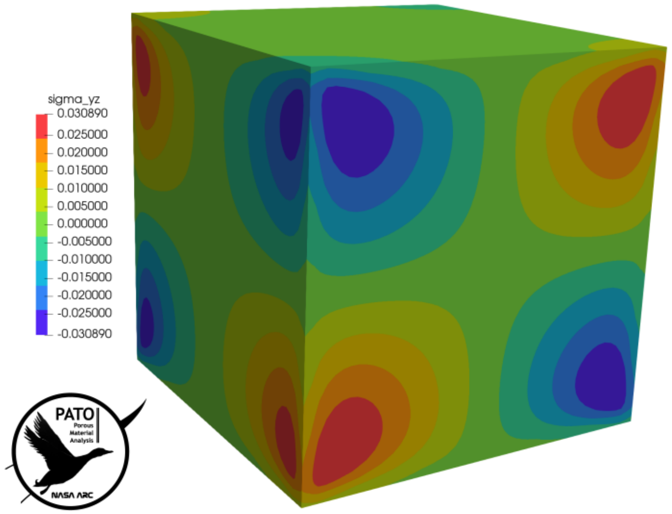

Failure Criteria and Mass Removal Model

Failure criteria model

- In the maximum stress failure theory [6], the maximum stresses of each mode are compared to the material strength using the following equation in 2D:

$$\max\left(\frac{\sigma_{xx}}{\mathrm{F}_{\mathrm{tu},xx}}, \left|\frac{\sigma_{xx}}{\mathrm{F}_{\mathrm{cu},xx}}\right|, \frac{\sigma_{yy}}{\mathrm{F}_{\mathrm{tu},yy}}, \left|\frac{\sigma_{yy}}{\mathrm{F}_{\mathrm{cu},yy}}\right|, \left|\frac{\sigma_{xy}}{\mathrm{F}_{\mathrm{su},xy}}\right|\right) > 1$$

- Where tu, cu and su are the maximum tension, compression and shear material strengths in x and y directions. σ_{ij} is the stress tensor computed in the stress analysis solver. The validity of this theory is further enhanced by the fact that spallation failure is expected to be brittle. An example is given here:

$\sigma_{xx} = 100$ kPa $\sigma_{yy} = 100$ kPa $\sigma_{xy} = 100$ kPa	$\sigma_{xx} = 2$ MPa $\sigma_{yy} = 100$ kPa $\sigma_{xy} = 100$ kPa	$\sigma_{xx} = 100$ kPa $\sigma_{yy} = 100$ kPa $\sigma_{xy} = 100$ kPa
$\sigma_{xx} = 100$ kPa $\sigma_{yy} = 100$ kPa $\sigma_{xy} = 100$ kPa	$\sigma_{xx} = 100$ kPa $\sigma_{yy} = 100$ kPa $\sigma_{xy} = 100$ kPa	$\sigma_{xx} = 100$ kPa $\sigma_{yy} = 100$ kPa $\sigma_{xy} = 100$ kPa

Ultimate strengths

$\mathrm{F}_{\mathrm{tu,xx}} = 1$ MPa

$\mathrm{F}_{\mathrm{cu,xx}} = 1$ MPa

$\mathrm{F}_{\mathrm{tu,yy}} = 1$ MPa

$\mathrm{F}_{\mathrm{cu,yy}} = 1$ MPa

$\mathrm{F}_{\mathrm{su,xy}} = 1$ MPa

Mass removal model

- The surface recession rate $\dot{s}$ and the mass loss M_{loss} due to mechanical erosion are computed as follows:

$$\dot{s} = \frac{L}{\Delta t} \qquad M_{\mathrm{loss}} = \rho\ A\ \dot{s}\ \Delta t$$

- Where L is the failing distance computed with a mesh search algorithm, Δt is the time step, ρ is the solid density, A is the surface area. The failing region is removed only if its topology is connected to the surface. The veloctityLaplacian motion solver implemented in OpenFOAM was used to move the dynamic mesh. An example is given here:

Failing distance using mesh search algorithm

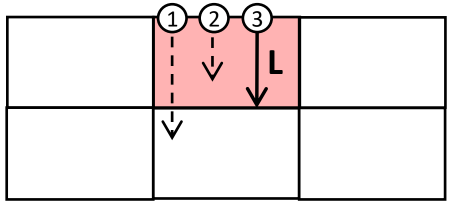

Mass removal using dynamic mesh motion

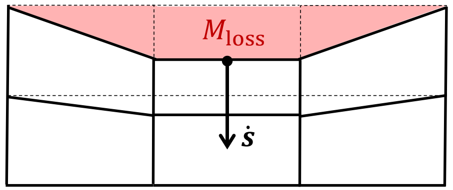

Conclusions and Future Work

- Described a methodology to carry out multi-scale analyses of TPS composites with PuMA to obtain the homogenized orthotropic mechanical properties.
  - Firstly, modeling the constituents at the micro-scale, and then using those results to accurately model the unit cell.
  - Results were validated for the porous matrix and the yarns of a 3D woven TPS by comparing them to semi-empirical expressions listed in the literature.
- Described the mechanical erosion model implemented in PATO to predict the mechanical response of TPS materials during atmospheric entry.
  - This model relies on having accurate TPS mechanical properties, which can be computed with PuMA.
  - The implemented stress analysis solver was validated against analytical expressions and FEA results.
  - Implemented a failure criteria and mass removal model that accounts for the potential mechanical erosion.

Future work:

- Validate the full-scale mechanical erosion model coupled with the rest of the entry physics against results obtained from arc-jet experiments.

References

[1] Ferguson, J. C., Semeraro, F., Thornton, J. M., Panerai, F., Borner, A., & Mansour, N. N. (2021). Update 3.0 to PuMA: The porous microstructure analysis software",(PII: s2352711018300281). SoftwareX, 15, 100775.

[2] Lachaud, J., & Mansour, N. (2013). Porous-material Analysis Toolbox based on OpenFOAM-extend and Applications. In 44th AIAA Thermophysics Conference (p. 2767).

[3] Nordbotten, J. M., “Cell-centered finite volume discretizations for deformable porous media,” International journal for numerical methods in engineering, Vol. 100, No. 6, 2014, pp. 399–418.

[4] Keilegavlen, E., and Nordbotten, J. M., “Finite volume methods for elasticity with weak symmetry” International Journal for Numerical Methods in Engineering, Vol. 112, No. 8, 2017, pp. 939–962.

[5] Omairey, S. L., Dunning, P. D., and Sriramula, S.,"Development of an ABAQUS plugin tool for periodic RVE homogenisation," Engineering with Computers, Vol. 35, No. 2, 2019, pp. 567–577.

[6] Andreassen, E., and Andreasen, C. S., "How to determine composite material properties using numerical homogenization," Computational Materials Science, Vol. 83, 2014, pp. 488–495

[7] Bert, C. W., “Prediction of elastic moduli of solids with oriented porosity,” Journal of materials science, Vol. 20, No. 6, 1985,pp. 2220–2224.

[8] Roberts, A. P., and Garboczi, E. J., “Elastic properties of model porous ceramics,” Journal of the American Ceramic Society, Vol. 83, No. 12, 2000, pp. 3041–3048.

[9] Ghafaar, M. A., Mazen, A., and El-Mahallawy, N., “Application of the rule of mixtures and Halpin-Tsai equations to woven fabric reinforced epoxy composites,” JES. Journal of Engineering Sciences, Vol. 34, No. 1, 2006, pp. 227–236.

[10] Halpin, J. C., “Effects of Environmental Factors on Composite Materials.” Tech. rep., Air Force Materials Lab Wright-Patterson AFB OH, 1969.

References

[11] Nielsen, L. E., “Generalized equation for the elastic moduli of composite materials,” Journal of Applied Physics, Vol. 41, No. 11, 1970, pp. 4626–4627.

[12] Chamis, C. C., “Simplified composite micromechanics equations for hygral, thermal and mechanical properties,” 1983.

[13] Meurisse, J. B. E., Lachaud, J., Panerai, F., Tang, C., & Mansour, N. N. (2018). Multidimensional material response simulations of a full-scale tiled ablative heatshield. Aerospace Science and Technology, 76, 497-511.

[14] Thornton, J. M., Meurisse, J. B. E., Fraile Izquierdo, S., Dias, B., Bellas Chatzigeorgis, G., and Mansour, N. N.. "Recent Advancements in the PATO Material Response Code", International Planetary Probe Workshop (2022)

[15] Schneider, P. J., T. A. Dolton, and G. W. Reed. "Mechanical erosion of charring ablators in ground-test and re-entry environments." AIAA Journal 6.1 (1968): 64-72.

[16] Cardiff, Philip, et al. "A large strain finite volume method for orthotropic bodies with general material orientations." Computer Methods in Applied Mechanics and Engineering 268 (2014): 318-335.

[17] Demirdžić, I., et al. "Finite volume analysis of stress and deformation in hygro-thermo-elastic orthotropic body." Computer methods in applied mechanics and engineering 190.8-10 (2000): 1221-1232.

[18] Lekhnitskii, Sergei Georgievich, et al. "Theory of elasticity of an anisotropic elastic body." Physics Today 17.1 (1964): 84.

[19] Toubal, Lotfi, Moussa Karama, and Bernard Lorrain. "Stress concentration in a circular hole in composite plate." Composite structures 68.1 (2005): 31-36.

[20] Cardiff, Philip. "Development of the finite volume method for hip joint stress analysis”. University College Dublin (2012).

[21] Oruganti, S., Fraile Izquierdo, S., Meurisse, J. B. E., Bellas Chatzigeorgis, G., and Mansour, N. N. "Inclusion of thermal expansion for orthotropic materials into PATO's stress analysis solver” (2022).

Thank You

Questions?

sergio.fraile.Izquierdo@nasa.gov